Digest Journal of Nanomaterials and Biostructures Vol. 20, No. 4, October-December 2025, p. 1437-1446

Structural features of single-crystal silicon with scandium and yttrium impurities

Kh. S. Daliev [a, *], Sh. B. Utamuradova [b], I. Kh. Khamidjonov [b]
[a] *Branch of the Federal State Budgetary Educational Institution of Higher Education "National Research University MPEI", 1 Yogdu st., Tashkent, Uzbekistan*
[b] *Institute of Semiconductor Physics and Microelectronics, National University of Uzbekistan,20 Yangi Almazor st., Tashkent, 100057, Uzbekistan*

This study investigates the structural characteristics of silicon doped with scandium and yttrium through X-ray structural analysis. The findings reveal that crystallites composed of SiSc, SiO_2, and Sc_2O_3 are predominantly concentrated in the near-surface regions of the sample, forming oxide layers with polycrystalline properties. These crystallites exhibit distinct space groups and crystallographic parameters: Sc_2O_3 has trigonal symmetry (a = b = 0.3412 nm, c = 0.5648 nm, α = β = 90°, γ = 120°, space group $P\bar{3}m1$), SiO_2 also has trigonal symmetry (a = b = 0.4998 nm, c = 0.5511 nm, α = β = 90°, γ = 120°, space group $P3_121$), and SiSc demonstrates cubic symmetry (a = b = c = 0.4413 nm, α = β = γ = 90°, space group $F\bar{4}3m$). Furthermore, the bulk regions of n-Si<Y> samples contain crystallites with varying crystallographic orientations and sizes, associated with diverse space groups. These include Y_2O_3 with tetragonal symmetry (a = b = 0.3819 nm, c = 0.5467 nm, α = β = γ = 90°, space group $P\bar{4}m2$), SiO_2 with trigonal symmetry (a = b = 0.4998 nm, c = 0.5511 nm, α = β = 90°, γ = 120°, space group $P3_121$), Si with cubic symmetry (a = b = c = 0.4413 nm, α = β = γ = 90°, space group $F\bar{4}3m$), and SiY with cubic symmetry (a = b = c = 0.4712 nm, α = β = γ = 90°, space group $Pm\bar{3}m$). The rapid cooling of Si<Y> samples induce the formation of unsaturated bonds, attributed to the absence of oxygen and yttrium atoms in the ordered arrangement of silicon-oxygen-yttrium atoms in certain polycrystalline regions.

(Received September 11, 2025; Accepted November 11, 2025)

Keywords: Silicon, Oxygen, Scandium, Yttrium, X-ray diffraction pattern, Subcrystallite, Nanocrystallite, Space group, Crystallographic orientation

1. Introduction

The incorporation of various elemental atoms into semiconductor materials is a crucial method for modulating their electrical, optical, and structural properties. Silicon (Si) plays a pivotal role in modern microelectronics due to its exceptional properties, including high carrier mobility and a wide energy bandgap. However, to enhance the performance of silicon-based devices and develop novel functional materials, it is essential to introduce foreign atoms into the silicon crystal lattice [1-6, 13-16].

Scandium (Sc) and yttrium (Y), as members of the rare earth metals group, are particularly intriguing for silicon doping due to their distinctive physical and chemical characteristics. The addition of Sc and Y atoms into the silicon lattice can significantly alter its electronic and structural properties, presenting opportunities for the development of highly efficient semiconductor devices. Specifically, doping with scandium and yttrium can influence key parameters such as electrical conductivity, charge carrier mobility, and material resilience under various external conditions.

X-ray diffraction studies of silicon doped with scandium and yttrium provide critical insights into how these impurities affect the crystal lattice. This includes analyzing changes in unit cell dimensions, the emergence of new phases or defects, and their impact on the material's physical properties and structural distortions. Understanding these modifications is crucial for

* Corresponding author: islomjon_xx@mail.ru
https://doi.org/10.15251/DJNB.2025.204.1437

advancing doped semiconductor technologies and unlocking potential applications in electronics and photonics.

This study presents the results of X-ray diffraction analysis of silicon doped with scandium and yttrium, focusing on changes in the crystal structure, the resulting defects, and distortions, and their implications for the functional properties of the material.

2. Experimental methodology

Single-crystal n-type silicon plates with a specific resistance of 100 Ω·cm, grown using the Czochralski method, served as the starting material. A known drawback of this growth technique is the relatively high concentration of background impurities, particularly oxygen and carbon, with levels up to 2×10^{18} cm^{-32} and 5×10^{16} cm^{-35}, respectively. The issue of oxygen impurities has remained a persistent challenge in silicon crystal growth over the past six decades.

Doping with scandium and yttrium atoms was achieved via gas-phase diffusion at 1200°C in evacuated quartz ampoules (10^{-4} Pa) for 10 hours, followed by controlled rapid and slow cooling processes. The structural and phase composition of the samples was analyzed using an Empyrean Malvern X-ray diffractometer. Peak maxima were determined with the OriginPro2019 software. X-ray diffraction measurements were conducted in the Bragg-Brentano geometry within a 2θ scattering angle range of 10° to 90°, at a continuous scan rate of 0.33°/min and an angular step size of 0.02°.

3. Experimental results and discussion

Figure 1 shows the X-ray diffraction pattern of the initial n-type silicon. The pattern reveals several structural reflections of varying intensities. The structural line observed at a scattering angle of 2θ = 27.99°, with d/n=3.188 nm, exhibits the highest intensity and corresponds to the crystallographic orientation (111). Its measured intensity (112,341 imp·s^{-1}) and half-width (0.005 rad) confirm the high crystallinity of the sample, with most constituent atoms organized in the (111) crystallographic arrangement.

The β component of this reflection appears at 2θ = 25.31° with d/n=3.5096. Additionally, the second (222) and third (333) order reflections occur at 2θ = 57.9° (d/n=1.5933 nm) and 2θ = 94.68° (d/n=1.0474 nm), respectively. While the second-order (222) reflection is typically forbidden relative to the first-order (111) crystallographic line, it appears in this pattern due to microdistortions in the crystal lattice. The intensity ratio I(222)/I(111)=3.6×10^{-3}, exceeding the threshold of 10^{-4}, further supports the presence of lattice microdistortions [6-12].

These microdistortions likely result from the uneven distribution of oxygen atoms, a major background impurity in silicon-based structures. Additional evidence for lattice distortions is seen in the non-monotonic inelastic background level of the X-ray diffraction pattern, which varies across small, medium, and large scattering angles. This variability suggests structural irregularities induced by the background impurities.

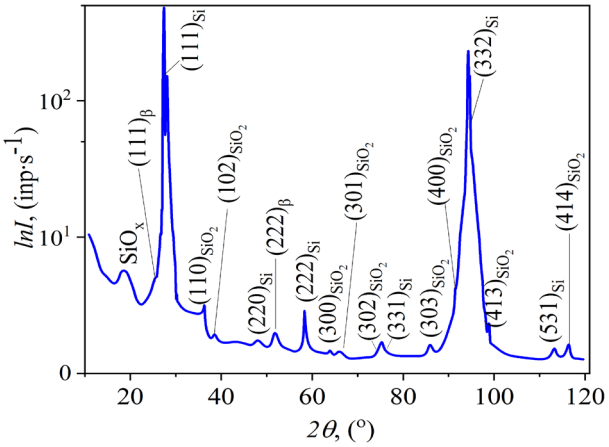

Fig. 1. X-ray diffraction pattern of the initial n-Si.

These microdistortions, resulting from the incorporation of multiple oxygen atoms into the crystal lattice with unsaturated silicon-oxygen bonds, contribute to the formation of a thin surface layer on the n-Si plate, which belongs to a different phase group. Consequently, the X-ray diffraction pattern at small and medium scattering angles reveals several structural lines ((110), (102), (300), (301), (302), (331), (303), (400), (413), (631), and (414)) that correspond to silicon dioxide.

The crystal lattice parameters were calculated using the experimental values of these structural reflections based on the formulas provided in [7]. The parameters were determined to be a=b=4.9762 nm and c=5.4321 nm, indicating that the unit cell belongs to a trigonal crystal lattice with the space group $P3_21$. Analysis of these results, along with the SiO_2 crystallite sizes listed in Table 1 and their various crystallographic orientations, confirms the formation of a polycrystalline layer approximately 1–2 μm thick on the surface of the n-Si plates. Additionally, the distinct splitting of the third (333) structural reflection into α_1 and α_2 components in the X-ray diffraction pattern, differing by a factor of two, suggests the presence of a surface layer formed due to microstresses.

The X-ray diffraction pattern at small scattering angles ($2\theta \approx 17.1^\circ$) reveals a broad diffuse reflection with a full width at half maximum (FWHM) of 0.12 rad. This reflection arises from structural fragments of SiO_x present in the near-surface layers, characterized by unsaturated bonds. The significant width of this reflection suggests that the structural fragments are small and lack long-range order in their arrangement. Consequently, these fragments are identified not as SiO_x nanocrystals but as clusters, with characteristic sizes of approximately 1.1 nm.

Additionally, based on the experimental values of the primary (111) structural reflection, the lattice parameter of the studied n-Si plate was determined to be a_{Si}=0.5456 nm

Figure 2(a) presents the X-ray diffraction patterns of n-Si platinum samples doped with Sc atoms for 10 hours at 1200 °C, followed by slow cooling. The diffraction pattern of the n-Si<Sc> samples shows significant differences compared to that of the undoped n-Si platinum samples depicted in Figure 1. Notably, the intensity of the main structural line (111) remains unchanged, whereas the intensities of the second (222) and third (333) order reflections increase by factors of 1.6 and 82, respectively [10-14].

The presence of the forbidden second-order (222) reflection and the intensity ratio $I(222)/I(111)=4.8\times10^{-3}$, which is significantly less than the threshold value of 10^{-4}, highlights notable changes in the crystal structure. Furthermore, the intensity of the third-order (333) reflection is 4.5 times greater than that of the main (111) reflection, indicating the formation of volume defects at subcrystallite interfaces. These defects likely result from the extended heat treatment of the samples and rapid cooling at the conclusion of the process.

Additionally, the main (111) structural line is shifted toward higher scattering angles ($\Delta\theta=0.18^\circ$) Experimental analysis of this structural line determined that the crystal lattice constant

of the doped sample is aSi<Sc>=0.5418 nm. This observation underscores the structural modifications induced by scandium doping under the specified conditions.

Additionally, the X-ray diffraction pattern reveals several structural reflections corresponding to different crystallographic orientations in the small and medium angle scattering ranges. The experimental and calculated data for these reflections are summarized in Table 1. Analysis of the results indicates that these reflections arise from the mutual ordering of SiSc, SiO_2, and Sc_2O_3 compounds.

The prolonged heat treatment of the samples facilitates the diffusion of Sc atoms, which interact with silicon and oxygen atoms, the latter originating from the primary background impurities in silicon, to form nanocrystallites. This formation is corroborated by the monotonic trend of the inelastic background level in the medium and large-angle scattering regions of the X-ray diffraction pattern for the n-Si<Sc> plate. These observations highlight the structural changes induced by scandium doping and prolonged heat exposure, which lead to the creation of ordered phases and nanocrystalline formations.

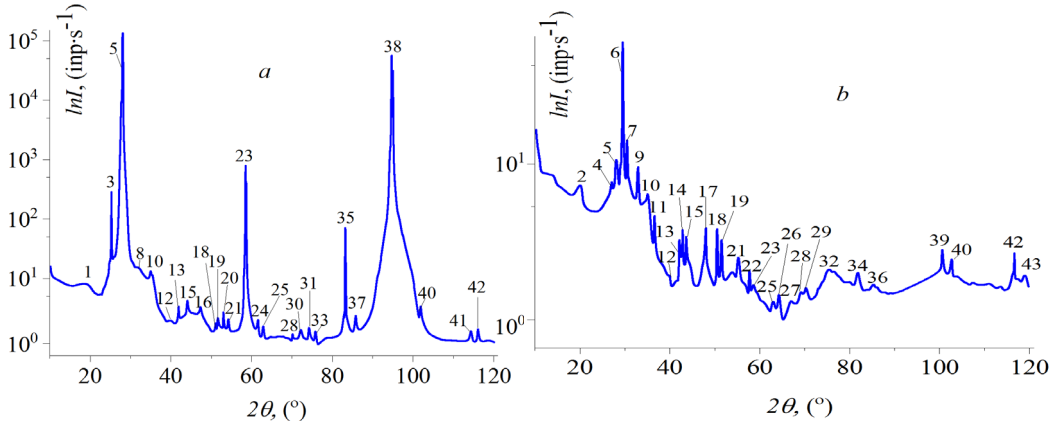

Fig. 2. X-ray diffraction pattern of n-Si doped with Sc atoms.

Following the experimental processes, including the slow cooling of the samples, it was determined that nanocrystallites composed of SiSc, SiO_2, and Sc_2O_3 compounds predominantly accumulate in the near-surface regions of the sample, forming oxide layers with polycrystalline properties. Analysis of the experimental results revealed that the nanocrystallites in this layer exhibit diverse crystallographic orientations and sizes, corresponding to distinct space groups:

- **Sc_2O_3**: Trigonal symmetry with lattice parameters a=b=0.3412 nm, c=0.5648 nm, α=β=90°, γ=120°, space group $P\bar{3}m1$.
- **SiO_2**: Trigonal symmetry with lattice parameters a=b=0.4998 nma = b = 0.4998,c=0.5511 nm, α=β=90°, γ=120°, space group $P3_121$.
- **SiSc**: Cubic symmetry with lattice parameters a=b=c=0.4413 nm, α=β=γ=90°, space group $F\bar{4}3m$.

Table 1. Structural data of n-Si doped with Sc atoms.

№	HKL	***n*-Si<Sc> 1200°C (*slow cool*)**		***n*-Si<Sc> 1200°C (*fast cool*)**	
		2Θ, (°)	I, (imp./c.)	2Θ, (°)	I, (imp./c.)
1.	SiO_x	18,88	8,28	10÷65	15,2÷1,2
2.	$(100)_{SiO_2}$	-		20,01	7,021
3.	$(111)_{SiSc}$ $(111)_{\beta}$	25,34	289	-	-
4.	$(101)_{SiO_2}$	-	-	26,72	7,38
5.	$(111)_{Si}$	28,15	129595	28,35	10,66
6.	$(200)_{SiSc}$	-	-	29,48	73,03
7.	$(100)_{Sc_2O_3}$	-	-	30,57	14,43
8.	$(002)_{Sc_2O_3}$	31,8	15,42	-	-
9.		-	-	33,04	9,5
10.	$(100)_{Sc_2O_3}$ $(2\bar{1}0)_{SiO_2}$	35,11	12,93	35,11	5,98
11.		-	-	36,68	4,62
12.	$(2\bar{1}1)_{SiO_2}$	40,09	2,93	39,94	2,53
13.	$(220)_{SiSc}$	41,83	3,96	42,06	3,78
14.		-	-	42,85	4,15
15.	$(102)_{Sc_2O_3}$ $(201)_{SiO_2}$	44,04	4,66	43,69	3,97
16.	$(220)_{Si}$	47,39	4,08	-	-
17.	$(311)_{SiSc}$	-	-	48,08	4,21
18.	$(222)_{\beta}$	50,95	2,73	50,6	4,16
19.	$(222)_{SiSc}$	51,58	3,14	51,44	3,8
20.	$(202)_{SiO_2}$	53,11	3,67	-	-
21.	$(2\bar{1}0)_{Sc_2O_3}$	54,4	3,05	54,28	3,19
22.	$(103)_{Sc_2O_3}$	-	-	57,75	2,67
23.	$(222)_{Si}$	58,49	811	58,74	2,21
24.	$(400)_{\beta}$	61,7	3,02	-	-
25.	$(200)_{Sc_2O_3}$	62,98	2,4	62,93	1,6
26.	$(300)_{SiO_2}$	-	-	64,21	1,85
27.	$(301)_{SiO_2}$	-	-	66,93	1,57
28.	$(400)_{Si}$	69,88	1,84	69,1	1,89
29.		-	-	70,38	2,1
30.	$(202)_{Sc_2O_3}$	72,209	2,25	-	-
31.	$(104)_{Sc_2O_3}$	74,13	2,46	-	-
32.	$(422)_{SiSc}$	-	-	75,35	2,77
33.	$(311)_{Si}$	76,06	2,05	-	-
34.	$(4\bar{3}1)_{SiO_2}$	-	-	81,78	2,63
35.	$(333)_{\beta}$	83,31	70,04	-	-
36.	$(303)_{SiO_2}$	-	-	85,52	2,55
37.	$(422)_{Si}$	86,87	3,39	-	-
38.	$(333)_{Si}$	94,81	55497	-	-
39.	$(2\bar{1}5)_{SiO_2}$	-	-	100,77	3,48
40.	$(5\bar{2}0)_{SiO_2}$	101,9	4,01	102,64	3,1
41.	$(531)_{Si}$	114,29	2,08	-	-
42.	$(4\bar{1}\bar{4})_{SiO_2}$	116,21	2,19	116,6	3,3
43.	$(205)_{Sc_2O_3}$	-	-	118,87	2,53

Scandium atoms were diffused into a silicon single crystal at 1200 °C for 10 hours, followed by rapid cooling at a rate of 300 °C/s. The resulting X-ray diffraction pattern is presented in Fig. 2(b). The diffraction patterns of the treated n-Si wafers exhibit significant differences compared to those of the initial samples (Fig. 1). Specifically, the intensity of the main structural reflection (111) decreases dramatically, by a factor of 10^5. However, the scattering angle for the (111) reflection remains nearly unchanged, with the lattice constant calculated as $a_{Si(pol)}$ = 0.5445, showing only a minor variation (Δa = 0.005 nm) from the original value. Notably, the second (222) and third (333) order reflections are absent from the diffraction pattern.

The rapid cooling process causes subcrystallites within the material to disintegrate, resulting in a reduction in their sizes, as shown in Table 2. The decrease in subcrystallite size increases the number of boundary regions, leading to a higher concentration of defective, high-potential areas, and microdistortions at the interfaces.

Additionally, rapid cooling facilitates the accumulation of nanocrystallites composed of SiO_2 and Sc_2O_3 compounds in the near-surface regions of the samples. These nanocrystallites form oxide layers characterized by polycrystalline properties, further altering the structural characteristics of the treated silicon wafers.

The X-ray diffraction pattern also revealed a structural line of relatively high intensity corresponding to the (200) reflection. Analysis of its experimental values confirmed that this line is associated with a silicon-scandium (SiSc) compound. The lattice constant and space group of the SiSc polycrystallite were determined based on the experimental data for this structural reflection.

The introduction of scandium atoms into the silicon single crystal at 1200 °C, followed by rapid cooling at a rate of 300 °C/s, resulted in a noticeable deterioration in the crystallinity of the samples. This process also led to the formation of polycrystalline spheres, which were identified as belonging to the SiSc, SiO_2, and Sc_2O_3 compounds. Additionally, the rapid cooling caused a reduction in subcrystallite sizes, further confirming the structural changes induced by this treatment. These observations highlight the impact of rapid thermal processes on the structural integrity and crystallographic properties of silicon doped with scandium.

Figure 3(a) presents the X-ray diffraction patterns of n-Si platinum samples doped with Y atoms for 10 hours at 1200 °C. The diffraction patterns of the n-Si<Y> samples differ markedly from those of the initial n-Si platinum samples shown in Figure 1. Notably, the intensity of the main structural reflection (111) decreases by a factor of 50. The presence of the forbidden second-order (222) reflection, with an intensity ratio I(222)/I(111) = $4.8*10^{-3}$ (significantly less than the threshold value of 10^{-4}), along with an intensity of the third-order (333) reflection three times higher than the main (111) reflection, indicates the formation of volume defects at subcrystallite interfaces. These defects likely arise from the prolonged heat treatment and rapid cooling applied during sample preparation.

Additionally, the main (111) structural line exhibits a shift toward higher-angle scattering ($\Delta\theta$=0.18◦). Based on experimental analysis of this structural line, the lattice constant of the doped sample was determined to be $a_{Si<Y>}$ = 5.4186 nm. This shift and change in lattice constant are attributed to the incorporation of Y atoms into the silicon crystal lattice. The difference in ionic radius of oxygen (r_o^{-2} = 1.3 Å)), yttrium (r_Y^{3+} = 0,91 Å), silicon (r_{Si}^{4+} = 0.42 Å and r_{Si}^{-4} = 2.7 Å) — leads to a lattice deformation of a_{Si} - a_{Si} - $a_{Si<Y>}$ = 0.026 nm, reflecting the structural distortions induced by the doping process.

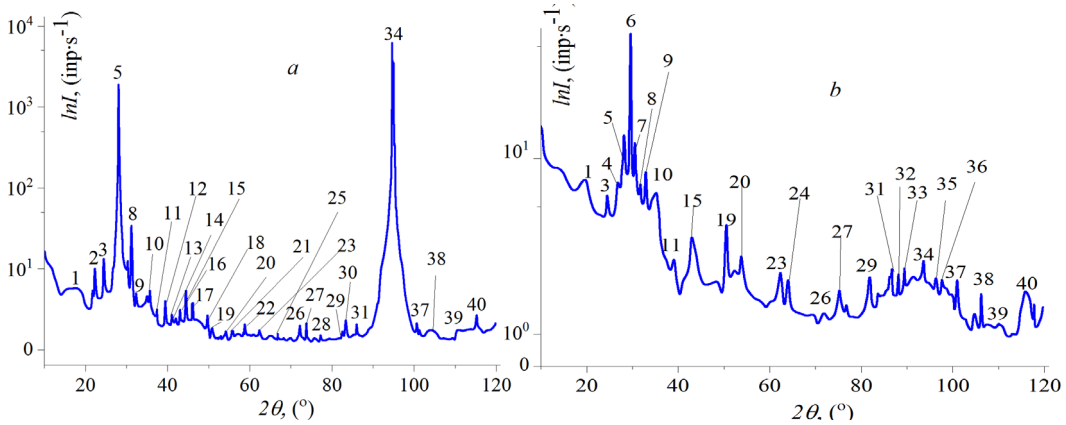

Fig. 3. X-ray diffraction pattern of n-Si doped with Y atoms.

The X-ray diffraction pattern of the n-Si<Y> samples at small and medium scattering angles reveals several structural reflections associated with different crystallographic orientations, as summarized in Table 2. Analysis of these results indicates that the observed reflections result from the combined ordering of SiY, SiO_2, and Y_2O_3 compounds.

During the prolonged heat treatment, diffusing yttrium atoms interact with oxygen atoms from the primary background impurities in the silicon, forming nanocrystallites. This process is reflected in the monotonic trend of the inelastic background level and the broader angular scattering observed in the X-ray diffraction pattern of the n-Si<Y> plate. Additionally, after rapid cooling, nanocrystallites composed of SiO_2 and Y_2O_3 compounds predominantly accumulate in the near-surface regions of the sample, forming oxide layers with polycrystalline characteristics.

The experimental data for the nanocrystallites indicate variations in crystallographic orientation and size, corresponding to distinct space groups:

- **Y_2O_3**: Tetragonal symmetry with lattice parameters a=b=0.3819 nm, c=0.5467 nm, α=β=γ=90°, space group $P\bar{4}m2$.
- **SiO_2**: Trigonal symmetry with lattice parameters a=b=0.4998, c=0.5511 nm, α=β=90°, γ=120°, space group P3121.
- **Si**: Cubic symmetry with lattice parameters a=b=c=0.4413 nma = b = c = 0.4413 nm, , α=β=γ=90°, space group $P\bar{4}3m$.
- **SiY**: Cubic symmetry with lattice parameters a=b=c=0.4712 nm, α=β=γ=90°, space group $P\bar{4}3m$.

Table 2. Structural data of n-Si doped with Y atoms.

№	HKL	***n*-Si<Y> 1200°C (a-samples)**		***n*-Si<Y> 1200°C (b-samples)**	
		2Θ, (°)	I, (imp./c.)	2Θ, (°)	I, (imp./c.)
1.	SiO_x	17,3	7.73	19.67	7.28
2.	$(101)_{SiO_2}$	22.13	9.6		
3.	111_{β}	24.54	1.56	24.4	5.9
4.	$(110)_{SiY}$			26.82	7.02
5.	111_{Si}	28.3	1910	28.3	13.61
6.	α_1-$(002)_{SiY}$			29.83	58.71
7.	α_2-$(101)_{SiY}$			30.62	12.15
8.	$(101)_{Y_2O_3}$	31.06	30.83	31.7	6.85
9.	$(111)_{SiY}$	33.04	6.79	32.89	8.14
10.	$(210)_{SiO_2}$ (2-1-10)	35.7	7.09	35.3	6.07
11.	$(200)_{SiY}$	38.47	4.85	38.86	3.28
12.	$(201)_{SiO_2}$ (2-1-11)	39.55	5.99	Å	
13.	$(102)_{Y_2O_3}$	40.98	4.28		
14.	$(200)_{SiO_2}$ (20-20)	41.77	4.12		
15.	$(210)_{SiY}$	42.9	4.92	43.15	4.056
16.	$(201)_{SiO_2}$ (20-21)	44.33	6.95		
17.	220_{Si}	46.91	5.7		
18.	$(202)_{SiO_2}$ (2-1-12)	49.6	4.19		
19.	$(201)_{Y_2O_3}$	51.04	2.47	50.45	4.32
20.	$(210)_{SiO_2}$ (20-22)	53.95	2.38	53.95	3.37
21.	311_{Si}	56.13	2.31		
22.	222_{Si}	58.74	3.32		
23.	$(210)_{SiO_2}$ (2-1-13)	62.54	2.47	62.34	2.84
24.	$(212)_{Y_2O_3}$			64.07	2.64
25.	$(210)_{SiO_2}$ (30-31)	66.73	2.03		
26.	$(104)_{Y_2O_3}$	72.16	3.12	72.06	1.65
27.	$(210)_{SiO_2}$ (30-32)	73.93	3.32	75.3	2.36
28.	$(301)_{Y_2O_3}$	77.43	1.89		
29.	$(400)_{SiY}$	82.35	3.54	81.78	2.74
30.	333_{β}	83,23	4,1		
31.	$(410)_{SiY}$	86.02	3.12	86.6	3.06
32.	$(312)_{Y_2O_3}$			88.14	2.91
33.	$(411)_{SiY}$			89.17	2.99
34.	333_{Si}	94.7	6220	93.66	3.56
35.	$(321)_{Y_2O_3}$			96.23	2.74
36.	$(421)_{SiY}$			97.91	2.59
37.	$(313)_{Y_2O_3}$	100.62	3.19	100.82	2.79

№	HKL	***n*-Si<Y> 1200°C (a-samples)**		***n*-Si<Y> 1200°C (b-samples)**	
		2Θ, (°)	I, (imp./c.)	2Θ, (°)	I, (imp./c.)
38.	$(210)_{SiO_2}$ (5-2-31)	103.98	2.45	104.72	1.61
39.	$(401)_{Y_2O_3}$	110.54	2.54	110.3	2.19
40.	$(314)_{Y_2O_3}$	115.32	4.05	115.67	2.41

Rapid cooling of the Si<Y> samples result in the formation of unsaturated bonds, caused by the incomplete incorporation of oxygen and yttrium atoms into the ordered silicon-oxygen-yttrium arrangement in certain polycrystalline regions (Fig. 3, b). This incomplete arrangement gives rise to small-sized clusters comprising a limited number of atoms [5-9]. The diminutive size and close proximity of these clusters contribute to the appearance of diffuse reflection observed in the small-angle scattering regions of the X-ray diffraction patterns for the studied samples. This diffuse scattering highlights the structural irregularities introduced by the rapid cooling process.

4. Conclusion

Consequently, following the procedures conducted under conditions of gradual cooling for n-Si<Sc> samples, it was determined that crystallites composed of SiSc, SiO_2, and Sc_2O_3 compounds predominantly concentrate in the near-surface regions of the samples, resulting in the formation of oxide layers characterized by polycrystalline properties. Based on the experimental results of a layer consisting of nanocrystallites of different crystallographic orientation and size, it was established that these nanocrystallites have different space groups (Sc_2O_3 – trigonal symmetry, a = b = 0.3412 nm, c = 0.5648 nm. α = β = 90°, γ = 120° Space group $P\bar{3}m1$, SiO_2 – trigonal symmetry, a = b = 0.4998 nm, c = 0.5511 nm. α = β = 90°, γ = 120° Space group $P3_121$, SiSc – cubic symmetry, a = b = c = 0.4413 nm, α = β = γ = 90°, Space group $F\bar{4}3m$). Thus, when introducing scandium atoms into a silicon single crystal at a temperature of 1200 °C and cooling at a rate of 300 °C/s, a deterioration in the crystallinity of the obtained samples was detected. The release of polycrystalline spheres was also observed and it was established that they belong to the compounds SiSc, SiO_2 and Sc_2O_3. It was noted that the size of the subcrystallites decreased with rapid cooling of the samples from high temperature. It was determined that crystallites with different crystallographic orientations and sizes were formed in the volume of *n*-Si<Y> samples. It was found that these crystallites have different space groups (Y_2O_3 – tetragonal symmetry, a = b = 0.3819 nm, c = 0.5467 nm. α = β = γ = 90 ° Space group $P\bar{4}m2$, SiO_2 – trigonal symmetry, a = b = 0.4998 nm, c = 0.5511 nm. α = β = 90 °, γ = 120 ° Space group $P3_121$, Si – cubic symmetry, a = b = c = 0.4413 nm, α = β = γ = 90 °, Space group $F\bar{4}3m$, SiY – cubic symmetry, a = b = c = 0.4712 nm, α = β = γ = 90 °, Pr.gr. $Pm\bar{3}m$). Rapid cooling of Si<Y> samples leads to the formation of unsaturated bonds due to the absence of oxygen and yttrium atoms in the ordered arrangement of silicon-oxygen-yttrium atoms of some polycrystalline regions.

References

[1] W.Heywang, K.H.Zaininger. Silicon: the Semiconductor Material. 1998. p.24-47.

[2] S. Z. Zainabidinov, Kh. S. Daliev, K. P. Abdurakhmanov, Sh. B. Utamuradova, I. Kh. Khomidjonov, and I. A. Mirzamurodov. The Influence of the Impurities with Deep Levels on the Iron Behavior in Silicon. Modern Physics Letters B, 1997, Vol. 11. №20, p. 909-912. https://doi.org/10.1142/S0217984997001110

[3] Sh.B. Utamuradova, Sh.Kh. Daliev, J.J. Khamdamov, Kh.J. Matchonov, M.K. Karimov, Kh.Y. Utemuratova, East Eur. J. Phys. 1, 276 (2025); https://doi.org/10.26565/2312-4334-2025-1-32

[4] Egamberdiyev, B.E, Xamidjonov, I.X, Mavlyanov, A.S, Amin o'g'li, S.S. International Journal of Engineering and Advanced Technology, 2019, 9(1), pp. 4813-4818. DOI: 10.35940/ijeat.A2929.109119

[5] Hocheon Yoo, Keun Heo, Md. Hasan Raza Ansari, Seongjae Cho. Anomaterials 2021, 11(4), 832; https://doi.org/10.3390/nano11040832

[6] K.S. Daliev, Sh.B. Utamuradova, J.J. Khamdamov, M.B. Bekmuratov, O.N. Yusupov, Sh.B. Norkulov, and Kh.J. Matchonov, East Eur. J. Phys. (4), 301-304 (2024); https://doi.org/10.26565/2312-4334-2024-4-33

[7]Sh.B. Utamuradova, Kh.J. Matchonov, J.J. Khamdamov, and Kh.Y. Utemuratova, New Materials, Compounds and Applications, 7(2), 93-99 (2023).

[8] K.Reivi, Defects and impurities in semiconductor silicon. / Ed. S.N. Gorin, trans. from English. - Moscow: Mir, 1984. - 475 p.

[9] S.Z. Zainabidinov, A.Y. Boboev, Physics and technology of multicomponent thin-layer heterostructures based on A3B5 semiconductors, Monograph, Fan, Tashkent. - 2022. - 120 p.

[10] S.Z. Zainabidinov, A.S. Saidov, M.U. Kalanov, A.Y. Boboev, Applied Solar Energy, (2019). 55(5).p.291-308; https://doi.org/10.3103/S0003701X1905013X

[11] Yu.M. Tairov, V.F. Tsvetnov, Technology of semiconducting and dielectric materials, Vysshaya shkola, 1990. 423 p. D.

[12] D.D. Avrov, O.A. Aleksandrova, A.O. Lebedev, E.V. Maraeva, Yu.M. Tairov, A. Yu. Fadeev. Technology of material microelectronics: ot mineralnogo syrya k monokristallu: ucheb. posobie. SPb.: Izd-vo SPbGETU "LETI", 2017. 146 p.

[13] V.M. Babich, N.I. Bletskan, E.F. Wenger, Oxygen and monocrystalline silicon, Kiev, Interpres LTD, 1997. - 240 p.

[14] G. Valikova, R.F. Vitman, A.A. Lebedov, S.K. Muhammedov. Boprosu o povedeni oxygen and silicon. //FTP, 1982. T.16, #12. S.2204 - 2206.

[15] A.N. Tereshchenko. Dislocatsionnaya luminescence in silicon with different primes composition. Candidate of Diss. phys.-math. science - Chernogolovka, 2011.162 p.

[16] Utamuradova Sh.B., Daliev Sh.Kh., Rakhmanov D.A., Khamidjanov I.Kh., DoroshkevichA.S., Mezentseva Zh.V., Tatarinova A. Influence of gamma rays on electrophysical properties of silicon doped with palladium atoms. Advanced Physical Research. Vol.7, No.3, 2025, pp.166-173. https://doi.org/10.62476/apr.73166